RESEARCH ARTICLE

Succession and potential role of bacterial communities during *Pleurotus ostreatus* production

Renáta Bánfi[1], Zsuzsanna Pohner[1,2], Attila Szabó[1], Gábor Herczeg[3], Gábor M. Kovács[4,†], Adrienn Nagy[5], Károly Márialigeti[1] and Balázs Vajna[1,*,‡]

[1]Department of Microbiology, Eötvös Loránd University, Pázmány Péter sétány 1/C, 1117 Budapest, Hungary, [2]Institute for Soil Sciences and Agricultural Chemistry, Centre for Agricultural Research, Herman Ottó út 15, H-1022 Budapest, Hungary, [3]Department of Systematic Zoology and Ecology, Eötvös Loránd University, Pázmány Péter sétány 1/C, 1117 Budapest, Hungary, [4]Department of Plant Anatomy, Eötvös Loránd University, Pázmány Péter sétány 1/C, 1117 Budapest, Hungary and [5]Pilze-Nagy Ltd., Talfája 50., H-6000 Kecskemét, Hungary

*Corresponding author: Department of Microbiology, Eötvös Loránd University, Pázmány Péter sétány 1/C, 1117 Budapest, Hungary. Tel: +36-1-372-25-00/8387; Fax: +36-1-381-2178; E-mail: vajna.balazs@ttk.elte.hu

One sentence summary: Bacterial community composition has changed significantly during *Pleurotus ostreatus* production, and this microbiome has a role in inhibiting competing microbes without affecting *P. ostreatus* growth.

Editor: Paolina Garbeva
†Gábor M. Kovács, https://orcid.org/0000-0001-9509-4270
‡Balazs Vajna, https://orcid.org/0000-0002-5604-7997

ABSTRACT

There is an increasing interest in studying bacterial-fungal interactions (BFIs), also the interactions of *Pleurotus ostreatus,* a model white-rot fungus and important cultivated mushroom. In Europe, *P. ostreatus* is produced on a wheat straw-based substrate with a characteristic bacterial community, where *P. ostreatus* is exposed to the microbiome during substrate colonisation. This study investigated how the bacterial community structure was affected by the introduction of *P. ostreatus* into the mature substrate. Based on the results obtained, the effect of the presence and absence of this microbiome on *P. ostreatus* production in an experimental cultivation setup was determined. 16S rRNA gene-based terminal restriction fragment length polymorphism (T-RFLP) and amplicon sequencing revealed a definite succession of the microbiome during substrate colonisation and fruiting body production: a sharp decrease in relative abundance of *Thermus* spp. and Actinobacteria, and the increasing dominance of Bacillales and *Halomonas* spp. The introduced experimental cultivation setup proved the protective role of the microbial community against competing fungi without affecting *P. ostreatus* growth. We could also demonstrate that this effect could be attributed to both living microbes and their secreted metabolites. These findings highlight the importance of bacterial-fungal interactions during mushroom production.

Keywords: Pleurotus ostreatus; T-RFLP; amplicon sequencing; bacterial community structure; bacterial-fungal interactions; succession and spatial heterogeneity

INTRODUCTION

The study of bacterial-fungal interactions (BFIs) has become increasingly important. Of particular importance is that BFIs can be considered as one of the simplest cross-kingdom (prokaryotic-eukaryotic models) interactions whose interplay has a major role in a number of fields, including nutrient cycling, host productivity, biocontrol, food production, and bioremediation (Deveau *et al.* 2018). One of the more specialised areas is wood colonisation and degradation (Johnston, Boddy and Weightman 2016), where white-rot fungi involved in the process may interact with bacteria in a variety of ways. Bacterial presence can have negative effects on fungi, as bacteria can rapidly consume easily degradable substrates (Messner *et al.* 2003); however, some bacterial products can serve as fungal growth factors (Clausen 1996). On the other hand, some white-rot fungi, such as *Hypholoma fasciculare* and *Resinicium bicolor*, decreased the number of wood-colonising bacteria, while the number of bacteria adhering to exploratory hyphae in the surrounding soil increased (Folman *et al.* 2008). Hervé *et al.* (2016) reported that *Phanerochaete chrysosporium* selected certain bacteria in its mycosphere during wood decay, which are less inhibitory to fungal growth and are involved in cellulose and hemicellulose degradation, and iron mobilisation. It is also possible that fungal species do not select bacteria directly, but rather indirectly through changing conditions during wood decay (Kielak *et al.* 2016).

Pleurotus ostreatus (oyster mushroom), a model organism for white-rot fungi, is the second most important cultivated edible mushroom in the world (Royse, Baars and Tan 2017) and has a remarkable role in bioremediation (Stella *et al.* 2017). Several studies have reported on the interactions between bacteria and *P. ostreatus*. *Pleurotus ostreatus* was reported to lyse bacterial colonies under low nutrient conditions (Barron 1988), decrease soil bacterial colony counts by several orders of magnitude (Lang *et al.* 1997), and kill most indigenous soil bacteria expected to take part in polycyclic aromatic hydrocarbon degradation (Gramss, Voigt and Kirsche 1999; Andersson *et al.* 2003). The antioxidant and antimicrobial (e.g. volatile compound production) properties of *P. ostreatus* (Beltran-Garcia, Estarron-Espinosa and Ogura 1997; Martínez *et al.* 2015; Smolskaite, Venskutonis and Talou 2015) may contribute to this impact. However, there are some examples of positive effects. Cho *et al.* (2003) demonstrated that fluorescent pseudomonads promoted the fruiting body formation of *P. ostreatus* on agar plates. Additionally, *P. ostreatus* appeared to stimulate bacterial growth in some cases (Stella *et al.* 2017), whereas Adamski and Pietr (2019) revealed at least 34 different bacterial genera living in association with eight *P. ostreatus* strains. Some of them had laccase-like genes, so these microorganisms could support the biodegradative capacity of *P. ostreatus*.

Notwithstanding the examples above, there is little information on the interactions between bacteria and *P. ostreatus* during mushroom production. The initial step of mushroom cultivation is the so-called substrate production. In Europe, a wheat straw-based substrate, prepared via partial composting, pasteurisation, and conditioning, is used (Rühl and Kües 2007; Vajna *et al.* 2012). First, the straw is moistened, and easily degradable substrates are consumed during partial composting. The elimination of easily degradable substrates hinders substrate contamination by competing microbes with no complete lignocellulose-degrading enzyme set during substrate colonisation of *P. ostreatus*. Also the accessibility of cellulose is increasing (Vajna *et al.* 2010). Second, pasteurisation eliminates competing and pathogenic microbes of *P. ostreatus*, and third, during

conditioning, the substrate is colonised with the surviving non-competing and non-pathogenic bacteria (Ororbia and Núñez 2001; Oei 2016). We previously described microbial succession during substrate preparation (Vajna et al. 2010, 2012). Fungal CFU (colony-forming unit) values reached their maxima during partial composting with species from genera *Thermomyces*, *Myceliophthora*, and *Rhizomucor* having versatile thermostable cellulolytic enzymes, suggesting their role in the initial straw polysaccharide decomposition (Vajna *et al.* 2010). Using sequence-aided terminal restriction fragment length polymorphism (T-RFLP), it was revealed that Proteobacteria (*Pseudomonas* and *Sphingomonas* spp.) dominated in the first phase of substrate preparation, Firmicutes (*Bacillus*, *Geobacillus*, and *Ureibacillus* spp.), *Pseudoxanthomonas*, and *Thermobispora* spp. at the end of partial composting, and several genera of Actinobacteria, *Thermus* spp., and Firmicutes (*Bacillus*, *Geobacillus*, *Thermobacillus*, and *Ureibacillus* spp.) in the mature substrate (Vajna *et al.* 2012).

P. ostreatus is exposed to this microbial community after spawning the mature substrate during substrate colonisation. However, it is not completely understood how microbial community structure changes during this process and what kind of interactions develop among microbial community members and *P. ostreatus*. Our first aim was to test using molecular fingerprint techniques and amplicon sequencing whether known bacterial community structure of the mature mushroom substrate was transformed during *P. ostreatus* production. Subsequently, a laboratory-scale experimental cultivation setup was established in which the effect of the presence and absence of microbiome on *P. ostreatus* cultivation was investigated. With the help of this system we addressed the following questions: (i) if microbes have any effect on *P. ostreatus* growth (ii) if there is an effect, whether it is attributed to the entire microbiome or to its extracellular metabolites (iii) a single indigenous bacterial strain could have an antagonistic effect on *P. ostreatus*? To monitor fungal functioning in the model, activity patterns of lignocellulose-degrading enzymes and hyphal growth rate were used as indicators.

MATERIALS AND METHODS

Bacterial community composition during large-scale production

Pleurotus ostreatus production and sampling

To study bacterial succession, samples derived from a large-scale *P. ostreatus* producer (Pilze-Nagy Ltd., Kecskemét, Hungary) were used as described previously (Bánfi *et al.* 2015). Briefly, mature mushroom substrate (after partial composting, pasteurisation, and conditioning) was inoculated with *P. ostreatus* HK35 spawn and filled into substrate blocks (22–25 kg; 55 × 35 × 20 cm). Blocks were incubated for substrate colonisation and subsequent fruiting body production in a temperature-, humidity-, and light-controlled production house. The cultivation cycle consisted of three main stages. First, *P. ostreatus* mycelia colonised the substrate blocks (24–26°C, 75–80% relative humidity [RH]); second, fruiting body production was induced (12–20°C, 85–90% RH); and third, mature fruiting bodies were produced and harvested (10–13°C, 75–80% RH). For further substrate utilisation and mushroom harvesting, a second cultivation cycle was applied (Fig. 1). The sampling period was 11 weeks from spawning (day 1) until the end of the second flush (day 71). Five mushroom substrate blocks ('A' to 'E') at different locations in a 250 m² production house were sampled: 30–30 g substrate was collected from surface layers (0–10 cm) of each block at
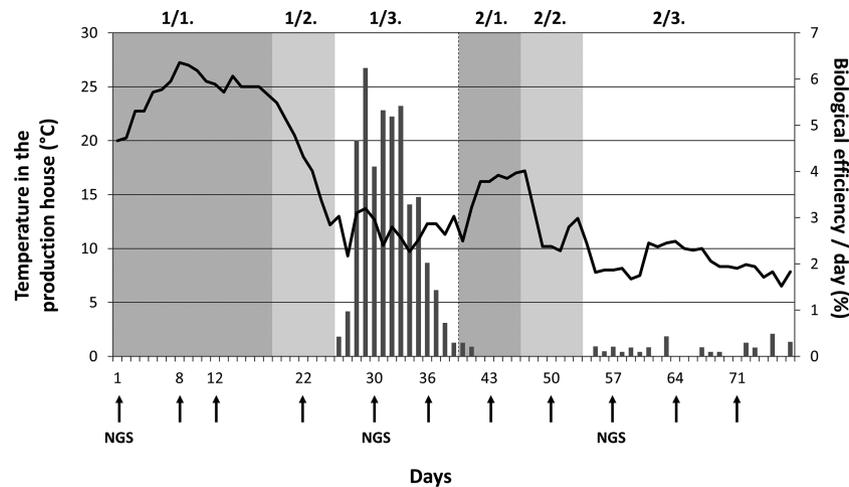
Figure 1. Stages of the *P. ostreatus* cultivation process and the 11 sampling days. Sampling days are denoted with numbers and arrows on the horizontal axis. 'NGS' shows samples processed for amplicon sequencing. Stage 1: 1/1. vegetative growth; 1/2. fruiting body induction; 1/3. first flush and harvest; Stage 2: 2/1. second vegetative growth; 2/2. second fruiting body induction; 2/3. second flush and harvest; columns: biological efficiency/day in the production house; black line: temperature during the investigation period. Biological efficiency was calculated as ratio of weight of fresh fruiting bodies per weight of dried substrate on day 1. Figure modified from Bánfi *et al.* (2015) with the permission of Fungal Biology.

three random regions to avoid the disturbance of the blocks. On day 71, blocks were cut in half, and the inner parts were sampled. Samples were stored at -20°C until further analysis.

T-RFLP analysis

DNA was extracted from the samples after grinding in liquid nitrogen as described by Vajna *et al.* (2010) using a G-spin™ Total DNA Extraction Mini Kit (iNtRON Biotechnology, Seongnam, South Korea). PCR reactions (using HEX-labelled 27F [5'-AGA GTT TGA TCM TGG CTC AG-3'] and 534R [5'-ATT ACC GGG GCT GCT-3'] 16S rDNA primers, Lane 1991), enzymatic digestion, purification of enzymatic digests, and electrophoresis of labelled fragments were carried out as previously described (Székely *et al.* 2009).

T-RFLP chromatograms were analysed using GeneMapper® Software v3.7 (Applied Biosystems, Foster City, CA, USA). Only T-RFs longer than 50 bp were used. Further data processing was performed according to an updated script of Abdo *et al.* (2006) (Supplementary Data). The following parameters were applied: noise filtration based on standard deviation (multiplier = 4) of peak area, and T-RFs alignment with a 1 bp clustering threshold. The resulting alignment was compared to raw chromatograms and manually corrected if needed. For normalisation, relative abundance of each detected T-RF within a given T-RFLP profile was calculated. To obtain a more robust result, the data matrix for *Alu*I and *Hin*6I enzymes was combined.

454 Pyrosequencing

To identify bacterial community members, selected samples (1–1 sample from blocks 'A' and 'B' at day 1, 30, and 57 corresponding to initial phase, first, and second flush) were subjected to pyrosequencing analysis. 16S rDNA library preparation, using the same primer pair as for T-RFLP, and sequencing were performed as described by Felföldi *et al.* (2015). Resulting sequence reads were processed as described by Szabó *et al.* (2017) using the Mothur v1.35 software (Schloss *et al.* 2009), SINA v1.2.11 aligner tool (Pruesse, Peplies and Glöckner 2012), and the ARB-SILVA SSU NR 99 reference database—SILVA Release 123 (Quast *et al.* 2013). Raw sequence reads are available in the NCBI Sequence Read Archive under BioProject ID PRJNA630385.

Phylogenetic composition of bacterial communities was visualised with the metacoder package of R software (R Core Team 2020; the used scripts are available as Supplementary Material).

Experimental cultivation setup

Preparation of the cultivation setup

To study the effect of the presence and absence of the microbiome, a *P. ostreatus* cultivation setup was established. 150 g of unspawned mature *P. ostreatus* substrate derived from the same production series as used for the large-scale production above were filled into tubes (30 cm, Ø 4 cm) formed from transparent plastic sheets (0.1 mm thick). Substrate density of the model tubes (∼0.6 kg/L) was the same as that in large-scale substrate blocks. Tube ends were covered with plastic foil. For gas exchange and fruiting body development, 15 holes (3 mm) were drilled evenly into the tubes (Fig. S1, Supporting Information).

Applied treatments are summarised in Fig. 2A. About 50 substrate-filled tubes were autoclaved at 121°C for 40 min. (i) Ten autoclaved tubes were used without any treatment, designated as 'A' namely 'autoclaved'. As autoclaving not only kills microbes but may also change the physicochemical structure of substrates (Berns *et al.* 2008), different inoculation treatments were used. (ii) First, a microbial suspension was prepared by adding 100 g of the same unspawned mature *P. ostreatus* substrate to 800 mL dechlorinated (0.1% w/v thiosulphate containing) sterilised tap water and shaken at 150 rpm at 28°C for 90 min. Ten autoclaved tubes were inoculated with the resulting microbial suspension, and each tube was injected under aseptic conditions with 10 mL of suspension evenly distributed through 15 holes (∼0.66 mL suspension/hole). The 10 tubes were designated as 'AM', namely 'autoclaved' substrate, and inoculated with 'microbial suspension'. (iii) To separate the effect of cells from their metabolites, cell-free extracts were prepared. Adequate volume of microbial suspension was filtered through a 0.2 μm cellulose nitrate membrane filter (Millipore, Billerica, MA, USA) to remove microbial cells. Then 10 mL of cell-free filtrate were used to inoculate 10 autoclaved tubes each in the same way as described above. Tubes were designated as
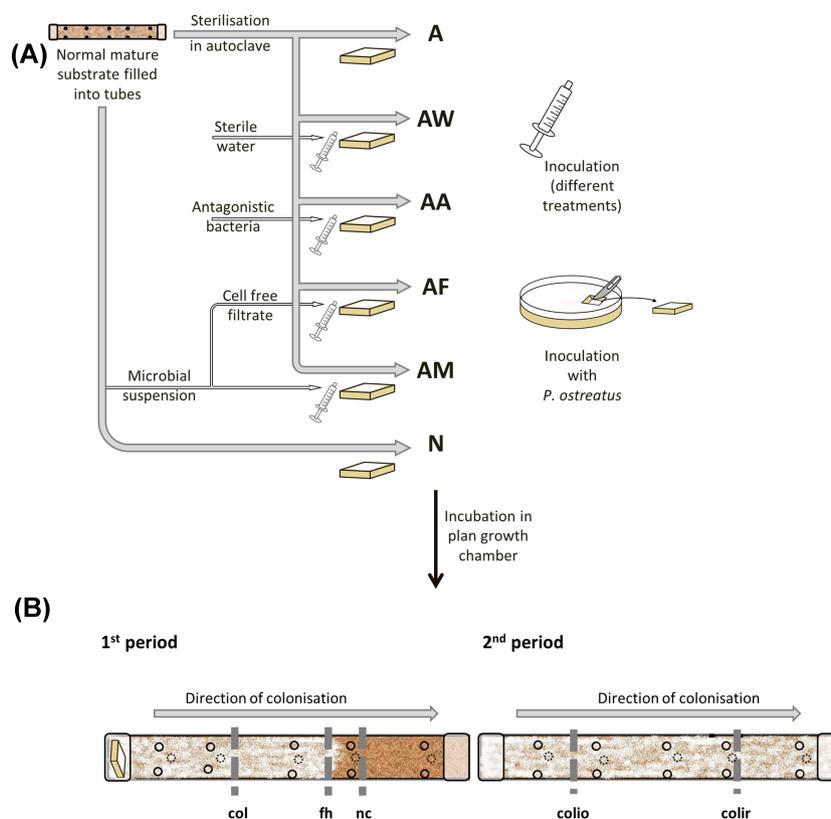
Figure 2. Scheme of applied treatments and sampling regions in the experimental cultivation setup. **(A)**, Scheme of applied treatments (see details in text and Supplementary Fig. 1) A: autoclaved; AW: autoclaved and sterile water injected; AA: autoclaved and inoculated with suspension of an antagonistic bacterium; AF: autoclaved and inoculated with cell-free filtrate of microbial suspension; AM: autoclaved and inoculated with microbial suspension; N: normal, untreated, not autoclaved. **(B)**, Sampling regions at the end of the 1st and 2nd periods of experiment. 'nc': noncolonised region, 'fh': region of front hyphae, 'col': three-week colonised region sampled before induction of the fruiting bodies, 'colio': older colonised region sampled after induction of fruiting bodies, 'colir': recently colonised region sampled after induction of fruiting bodies.

'AF', namely 'autoclaved' substrate and inoculated with cell-free 'filtrate' of microbial suspension. (iv) A bacterial strain collection from a mature *P. ostreatus* substrate was established previously. Strains were tested in simple cross-streak antagonism experiments with *P. ostreatus* on malt extract peptone agar (MEPA, DSMZ Medium 90) plates. Some of them showed inhibitory effects on *P. ostreatus* hyphal growth. To test the effect of a single antagonistic strain on *P. ostreatus* in our cultivation model, a suspension from one of the mentioned antagonistic strains (*Bacillus* sp. Sz55, 16S rRNA gene sequence GenBank accession number MK908096) was prepared in dechlorinated sterilised tap water with 0.04 OD_{600} density. Further, 10 mL of this suspension was inoculated into another 10 autoclaved tubes each, in the same way as described above. Tubes were designated as 'AA', namely 'autoclaved' and inoculated with the suspension of an 'antagonistic' bacterium. (v) To have an inoculation control, each of the 10 autoclaved tubes were injected with 10 mL of dechlorinated sterilised tap water, in the same way as above. These tubes were designated as 'AW', namely 'autoclaved' and inoculated with sterile 'water'. (vi) Finally, 10 tubes designated as 'N' were not autoclaved and contained normal, untreated mature *P. ostreatus* substrate. The fungal inoculum *Pleurotus ostreatus* strain HK35 (obtained from Sylvan Hungary Ltd.; Dunaharaszti, Hungary) was grown on MEPA plates at 28°C for one week. Thereafter, one end of cultivation model tubes was inoculated with a 2 × 2 cm hypha-covered MEPA culture block (Fig. 2A). Further, additional control tubes not inoculated with

P. ostreatus were produced, three tubes for treatment 'A', 10 for 'AM', 10 for 'AA', and two for 'N'.

Incubation and sampling of the tubes

All cultivation model tubes were placed in a plant growth chamber (Sanyo MLR-352H, Japan). In the 1st period, they were incubated for four weeks at 26°C and 90% RH without light, with partial aeration. Hyphal colonisation speed was recorded weekly by measuring the hyphal front distance from the inoculated end of the tubes. The position of the hyphal front was clearly visible by naked eye (Fig. S1, Supporting Information). Despite keeping the tubes in a 'clean environment', mould infection was observed during incubation around the tube holes. Contamination of the tubes was recorded at the end of the 1st period (at the end of the 4th week) by counting the number of contaminated and uncontaminated holes. To have colonised and still noncolonised parts in every tube, half of the tubes (i.e. 5 tubes from each of the six treatments: A, AM, AF, AA, AW, and N) were opened at the end of the 1st period, when one-third of every tube was still noncolonised (Fig. 2B). Additionally, half of the control tubes (not inoculated with *P. ostreatus*) were opened. Samples (10 g of each) were taken from three regions (non-colonised, front hyphae regions, and three-week colonised regions, Fig. 2B) of 30 *P. ostreatus* inoculated tubes and from two parts of control tubes. Samples were processed immediately for enzyme assays. In the 2nd period, the remaining tubes were incubated under the same conditions for two weeks until complete colonisation of

the tubes. The temperature was then decreased by 1.5°C/12 h until 16°C. At this temperature, fruiting body formation was induced by 12-hour light-dark cycle for two weeks. At the end of the 2nd period, the remaining 5 tubes from each of the six treatments and the other half of the control tubes were opened and 10 g of each samples were taken from two regions (recently and longer-colonized regions, Fig. 2B) of the 30 *P. ostreatus* inoculated tubes, and from two parts of the control tubes. Samples were processed immediately for enzyme assays.

Enzyme assays

Samples from model tubes were subjected to enzyme analysis according to Bánfi *et al.* (2015). Briefly, lignocellulolytic enzymes were extracted from 3 g of wet samples in 48 mL of 50 mM phosphate buffer (pH 7) with orbital shaking (100 rpm min^{-1}) at 8°C for 2 h. The extract was filtered through a VWR Collection (USA) no. 413 filter paper. The filtrate was used for enzyme activity measurements. Laccase activity was determined using ABTS (2,2'-azino-bis[3-ethylbenzothiazoline-6-sulfonic acid]; Sigma-Aldrich, USA), and manganese peroxidase (MnP) with DMAB-MBTH (3,3-dimethylaminobenzoic acid; Sigma-Aldrich, USA; 3-Methyl-2-benzothiazolinone hydrazone; Sigma-Aldrich, USA) as a substrate. Cellobiohydrolase, β-glucosidase, 1,4-β-xylosidase, and N-acetyl-β-glucosaminidase activities were assayed using p-nitrophenyl substrates (p-nitrophenyl-β-D-cellobioside [pNPC], p-nitrophenyl-β-D-glucoside [pNPG], p-nitrophenyl-β-D-xyloside [pNPX], and p-nitrophenyl-N-acetyl-β-D-glucosaminide [pNPN], respectively; Sigma-Aldrich, USA; Glycosynth, UK). Endo-β-glucanase (cellulase) and endo-1,4-β-xylanase activities were analysed using chromogenic substrates AZO-CM-CELLULOSE and AZO-XYLAN (Megazyme, Ireland), respectively. Spectrophotometric measurements were performed using a microplate reader (Sunrise, Tecan, Switzerland) and a UV-VIS spectrophotometer (Lambda35, PerkinElmer, USA). One unit of enzyme activity was defined as the amount of enzyme releasing 1 μmol of reaction product per minute. Results were calculated as units per gram of dry mass of the *P. ostreatus* substrate. Dry matter (DM) content was determined by drying the substrate samples at 105°C for 24 h.

Isolation and identification of infectious fungi

From visually different infected parts of the tubes, pure cultures were isolated on MEPA medium. For DNA extraction, a loopful of fungal culture was added to 100 μL 0.1 M Tris buffer (pH 8) containing 100 μL sterile glass beads (0.1 mm). The suspension was shaken in a mixer mill (Mixer Mill MM301, Retsch, Haan, Germany) at 30 Hz for 1 min. Crude lysates were heated at 98°C for 5 min and then centrifuged at 10 000 g for 5 min. The supernatant was used as a template for amplification of the fungal nrDNA ITS region with primers ITS1F forward [5'-TCC GTA GGT GAA CCT GCG G-3'; Gardes and Bruns 1993] and ITS4 reverse [5'-TCC TCC GCT TAT TGATAT GC-3', White *et al.* 1990]. Sanger sequencing of the amplicons was carried out by LGC Genomics (Berlin, Germany). Sequences were deposited in GenBank under accession numbers MW365370-MW365376 and were compared with sequences in public databases using BLASTn searches (Altschul *et al.* 1990).

Statistical analyses

Statistical analyses were performed using R software (R Core Team, 2020; the used scripts are available as Supplementary Material).

During interpreting bacterial T-RFLP dataset, the following analyses were carried out: (i) For comparing within and among block heterogeneity at selected sampling dates (day 1, 30, and 57), permutational multivariate analysis of variance using Bray-Curtis distances was carried out. Based on this result (see Supplementary Material), only one parallel sample from each block (11 sampling dates, one-one sample from the five mushroom blocks at each date) was used. (ii) Succession of the bacterial community was visualised using non-metric multidimensional scaling (NMDS) using Bray-Curtis distances. (iii) To test whether *a priori* grouping of samples according to sampling dates were separated significantly from each other, combined cluster and discriminant analysis (CCDA, Kovács *et al.* 2014; Bánfi *et al.* 2015) was applied. (iv) To test whether surface and inner samples of the same block at day 71 were different, two groups were compared with permutational multivariate analysis of variance using Bray–Curtis distances. To reveal how groups of inner samples were grouped with other samples, CCDA and NMDS with Bray-Curtis distances were used. Based on this result (see Supplementary Material) samples from the surface layers adequately represent bacterial community changes in the whole substrate block. (v) Shannon diversity indices were calculated. (vi) Spatial and temporal changes in community composition were calculated. Spatial heterogeneity was characterised on the cultivation block level using Bray–Curtis distances among samples within one sampling date. Weekly temporal changes were calculated using Bray-Curtis distances among samples from consecutive sampling dates. Differences among groups were tested using Kruskal-Wallis and Nemenyi *post-hoc* tests. (vii) To test the effect of *P. ostreatus* lignocellulose-degrading enzymes on bacterial community composition, enzymatic activities of the same samples were fitted as vectors onto the NMDS ordination, and the significance of fittings was tested with random permutations. Enzyme activity data was derived from Bánfi *et al.* (2015). (viii) Finally, for comparison, an already published T-RFLP dataset (Vajna *et al.* 2012) from the first part of the *P. ostreatus* mushroom production (Supplementary Fig. 2) was involved. That part is the so-called substrate production, from where the mature substrate used in this study was also gained.

For the cultivation model, the following statistical analyses were carried out: (i) Effect of treatments (A, AM, AF, AA, AW, and N) on the speed of hyphal colonisation was tested with a general linear model (LM) using generalised least squares with contamination of the tubes as covariant. The effect of the treatments on substrate contamination was also tested the same way. Based on the results of the later model (see Results and Discussion), a new explanatory variable was introduced as 'treatment type' with two categories for treatments with higher (A, AA, and AW) and lower (AM, AF, and N) contamination values. (ii) The effects of different treatments on enzymatic activities were tested separately for the two periods, as in the 1st and the 2nd periods in our cultivation model, different sets of model tubes were used due to destructive sampling. To create new summary variables from enzymatic activities, principal component analysis (PCA) using variance-covariance matrix was carried out on range standardised values separately for samples from 1st and 2nd periods. Only principal components, supported by the broken stick model, were used in further tests. For each principal component, enzyme activities with loadings above 0.53 or below -0.53 were considered for interpretation (Tabachnick and Fidell 2013). Effects of treatment, region, contamination, and treatment type on these new summary variables and with tube number as random effects was tested with general linear mixed-effects models (LMM). Random effect was used to control non-independence of

different regions sampled from the same tubes. The best models were found by automated model selection using combinations of fixed effect terms in original models and comparing them based on the Akaike information criteria. For both cases (i and ii), adjusted means were calculated, and *post-hoc* Tukey's tests were performed.

RESULTS AND DISCUSSION

Bacterial community composition during large-scale production

Bacterial community succession based on T-RFLP
In the first part of the study, samples were collected from a large-scale *P. ostreatus* producer (11 sampling days, five mushroom blocks with three parallel samples; Fig. 1). 16S rRNA encoding gene based T-RFLP fingerprints of the bacterial community showed a definite succession during 11 weeks of cultivation with the following significantly different groups of samples: day 1, day 8, day 12, day 22–30-36–43, and day 50–57-64–71 (Fig. 3A and Fig. S3, Supporting Information). Bacterial community diversity decreased slightly, based on Shannon indices (Fig. S4, Supporting Information). Spatial heterogeneity of samples within one sampling day was similar during the whole investigated period, whereas weekly shifts (Bray–Curtis distances among samples from consecutive sampling dates) decreased significantly during mushroom production (Fig. S5, Supporting Information), denoting the slowing of changes in the bacterial community. These rates of changes are easier to interpret when compared to the first part of *P. ostreatus* production, the so called substrate production (Fig. S2, Supporting Information) described by Vajna *et al.* (2012), where only during 12 days, but under more varied circumstances a much more remarkable change in the bacterial community was observed (Fig. 3C).

Substrate colonisation and fruiting body formation by *P. ostreatus* had the main influence on the bacterial community. Colonising hyphae produce high amounts of laccases, a known phenomenon when *P. ostreatus* interacts with other microorganisms (Baldrian 2004; Velázquez-Cedeño *et al.* 2008; Janusz *et al.* 2020). This could partially be responsible for changes in bacterial community composition in the first two weeks (Fig. 3B), although it is unclear whether laccases have a direct inhibitory effect on microbial growth (Baldrian 2004). Periodically decreasing temperature, ~25°C during substrate colonisation and 12–20°C during fruiting body production (Bánfi *et al.* 2015), and a rapid drop in pH from ~7 to ~5 (Viziteu 2004; De Boer *et al.* 2010) can have a strong effect on the bacterial community. Change of pH is a known process during wood degradation by which fungi control the environment and indirectly bacterial diversity (Johnston *et al.* 2019). From the third week, high activity of manganese peroxidase and different cellulases were significantly correlated with the transformation of bacterial community structure (Fig. 3B).

Bacterial community composition based on 454 pyrosequencing data
The 16S rRNA gene amplicon sequencing of 6 selected samples (1–1 sample from blocks 'A' and 'B' at day 1, 30 and 57) resulted in a total of 39094 high-quality reads classified within the domain Bacteria. Sequences were randomly subsampled according to the lowest number of sequences in sample block 'A' at day 30 (2994 sequences). Sequencing efficiency was high, with Good's coverage values ranging from 0.979 to 0.994. Observed number of OTUs and Shannon diversity indices showed a slight decrease in both blocks (Fig. 4, Table S1, Supporting Information).

Dominant trends in the bacterial community change during substrate colonisation and fruiting body production were the disappearance of *Thermus* spp., probably due to lower temperatures, a sharp decrease in Actinobacteria relative abundance, and an increase in members of the order Bacillales and *Halomonas* spp. (Fig. 5; Table S2, Supporting Information). The number of unclassified sequences (order level) decreased from 9%–12% to 1%–2% (Table S2, Supporting Information). Most of the dominant Bacillales genera (*Thermobacillus* and *Ureibacillus*) have already been described from the mature substrate of *P. ostreatus* production (Vajna *et al.* 2012). *Bacillus*, *Paenibacillus*, and *Lysinibacillus* spp. were also the main isolates identified from the *P. ostreatus* substrate described by Suarez *et al.* (2019). Many *Bacillus* spp. produce antifungal peptides (e.g. fengycin) with selective antagonistic ability as they inhibit green-mould disease causing *Trichoderma* spp. growth without affecting *P. ostreatus* (Kim *et al.* 2008; Nagy *et al.* 2012; Liu *et al.* 2015). *Paenibacillus polymyxa* also supports the competitiveness of *P. ostreatus* (Velázquez-Cedeño *et al.* 2008). Moreover, the thick gram-positive cell wall and spore forming potential of these Bacillales may enable their survival. Stella *et al.* (2017) reported a similar shift due to *P. ostreatus* toward the dominance of Firmicutes and disappearance of Actinobacteria in a polychlorinated biphenyl degrading soil community. Also in *Agaricus bisporus* production increasing ratio of gram-positive to gram-negative taxa was observed, suggesting selective suppression of different bacteria (Vos *et al.* 2017). The genus *Halomonas* contains moderately halophilic bacteria with broad pH (5–10) and temperature (10–45°C) tolerance (De La Haba *et al.* 2014), a compact cell wall (Vreeland, Anderson and Murray 1984), and exopolysaccharide production (Mata *et al.* 2006). Salt concentration of *P. ostreatus* compost was lower than *Agaricus* compost (Jasińska 2018), but the lower temperature (5–15°C) after the first fruiting body induction at day 22 might support their growth. Moreover, *Halomonas* spp. are highly abundant during denitrification and lignocellulose degradation in salty environments (Cortes-Tolalpa *et al.* 2018; Deng *et al.* 2020; Zhong *et al.* 2020), which might contribute to lignocellulose degradation during mushroom production.

### Effect of microbial presence on the cultivation of *Pleurotus ostreatus*

Monitoring of large-scale production provided an overview of the bacterial community composition, but the role and function of this community was unknown. The *P. ostreatus* cultivation model was developed to study the effect of the presence and absence of microbes.

#### Growth of P. ostreatus and contamination of the model tubes
The different applied treatments A, AW, AA, AF, AM and N (Fig. 2A) had a significant influence on colonisation speed (LM: $F_{5,54} = 6.78$, $P < 0.0001$). Although *P. ostreatus* can be produced on a sterilised substrate (Kwon 2004; Oei 2016), *P. ostreatus* grew significantly slower in autoclaved substrate with no additional treatments (A) and in autoclaved inoculation control (AW), than in normal (N) tubes (Fig. 6A, see Supplementary data). During weekly checking of the model system, mould infection was detected around the tube holes. According to nrDNA ITS sequences, those fungi belonged to the genera *Aspergillus* and *Penicillium*. Although the ITS region is not suitable for precise species identification in these groups, we assumed that three *Aspergillus* spp. and two *Penicillium* spp. were isolated. Moulds in both genera are common indoor fungi and can be found as competitors during mushroom production (Sağir and Yildiz 2004;
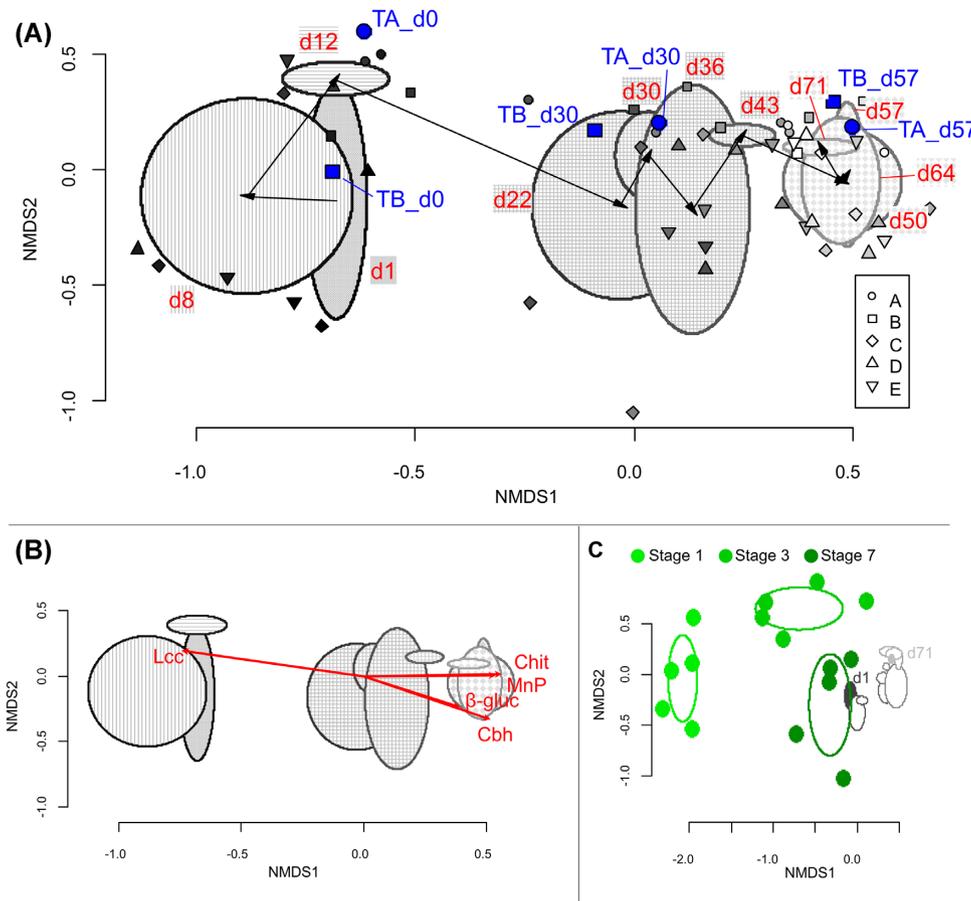
Figure 3. Bacterial community composition changes according to 16S rRNA gene based T-RFLP fingerprints during substrate colonisation and fruiting body production of P. ostreatus. **(A)** NMDS ordination using Bray-Curtis distances for samples. Different small symbols denote samples from different mushroom blocks (A–E). Filling of symbols is lightened from black to white in parallel with sampling date (day 1 to day 71). Blue filling shows samples subjected to pyrosequencing. Ellipses mark weekly mean ± SD area based on samples' NMDS coordinates; whereas, arrows point from weekn mean to weekn+1 mean. Filling of ellipses and their respective sampling date label denote significantly different groups of samples according to CCDA method (Supplementary Fig. 3). **(B)** The same NMDS ordination as in Fig. 3A though only ellipses for each week are plotted. Red arrows show significantly fitted (p < 0.05) P. ostreatus lignocellulose-degrading enzyme activities of the same samples. Enzyme activity data are derived from Bánfi *et al.* (2015). Enzyme names are abbreviated: β-gluc- β-glucosidase, Cbh- cellobiohydrolase, Chit- N-acetyl-β-glucosaminidase, Lcc-laccase, and MnP- manganese peroxidase. (C) NMDS ordination comparing bacterial community changes in P. ostreatus substrate preparation production series (data derived from Vajna *et al.* 2012) and samples from the present study. Substrate preparation is the first part of the P. ostreatus mushroom production, where the mature substrate also used in this study was produced. Ellipses correspond to mean ± SD area as in the previous parts. Stages 1, 3 and 7 in darkening green colours correspond to (S1) chopped, wetted wheat straw, (S3) end of partial composting, and (S7) mature substrate (Fig. S2, Supporting Information). For samples from the present study, only weekly ellipses of Fig. 3A are plotted.
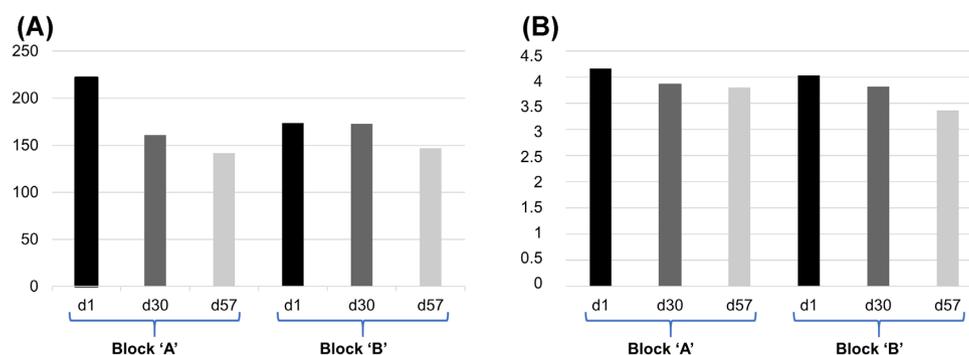
Figure 4. Bacterial diversity based on 16S rRNA gene amplicon sequencing during substrate colonisation and fruiting body production of *P. ostreatus* **(A)** Observed number of OTUs and **(B)** Shannon diversity calculated from the OTU (defined at 97% similarity level) numbers.
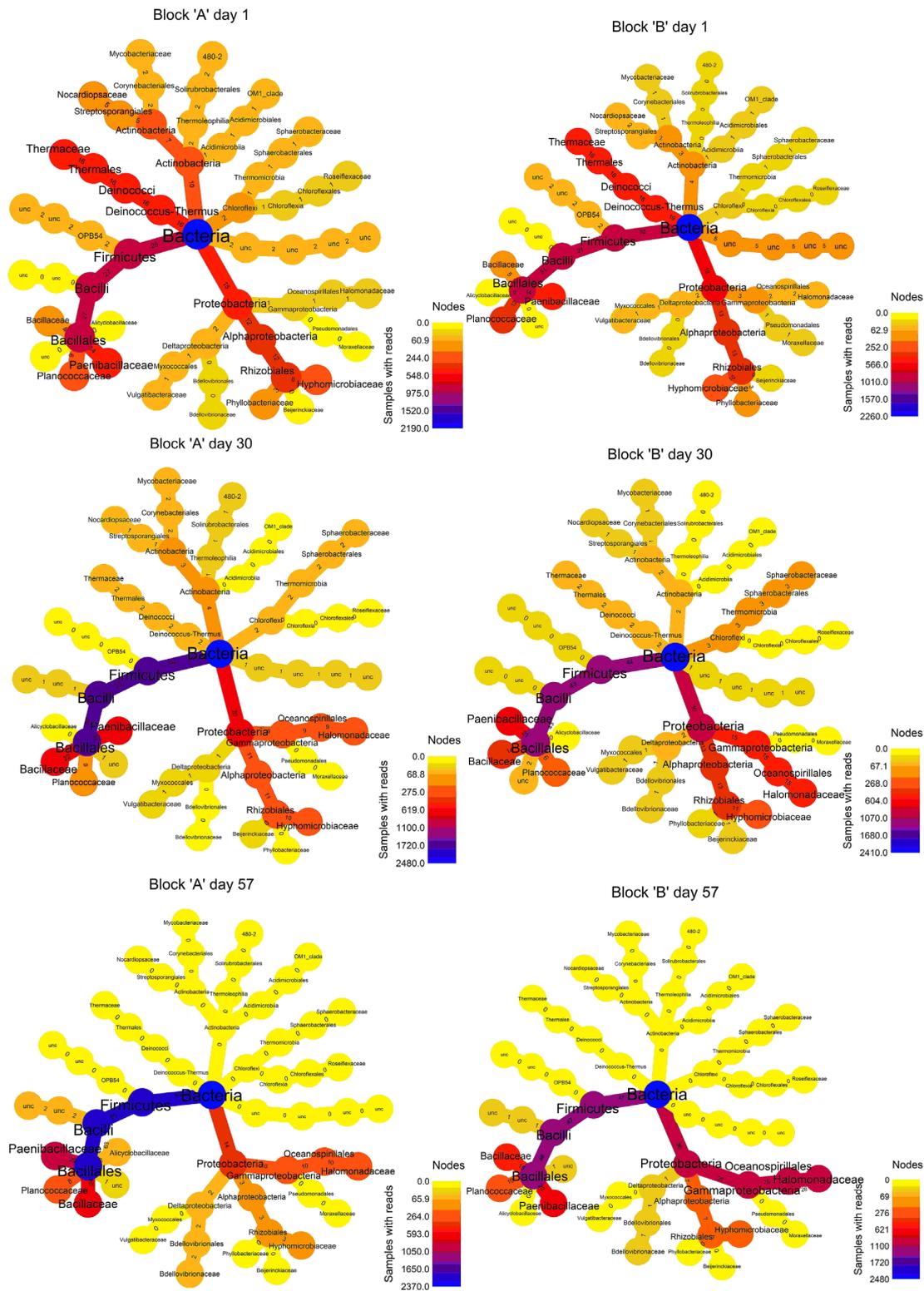
Figure 5. Phylogenetic composition of bacterial communities based on 16S rRNA gene amplicon sequencing during substrate colonisation and fruiting body production of *P. ostreatus*. Each node represents a taxon from kingdom to family. Tree topology is the same for every sample, whereas colour of the nodes goes from blue (100% relative abundance) through red to yellow (0% relative abundance) according to taxa abundance in each sample. Small numbers on the edges give relative abundance of the taxa, which follow the given edge. Only OTUs having >1% relative abundance at least in one sample were used for calculations. 'unc' stands for unclassified bacteria. The original size figure also complemented with genus level is available as Fig. S6 (Supporting Information).
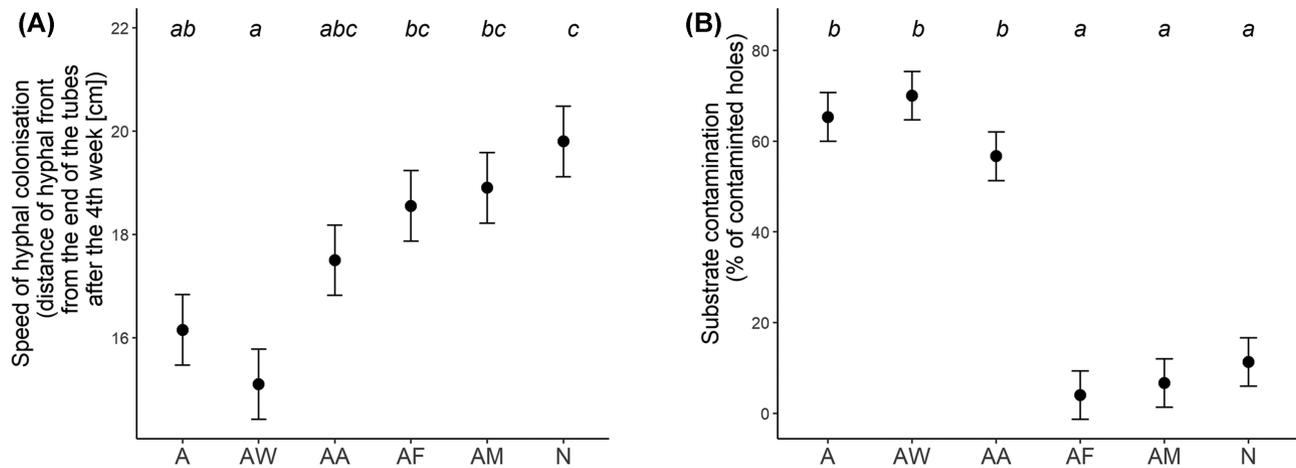
Figure 6. Effects of different treatments (for codes see Fig. 2A) on the **(A)** speed of P. ostreatus hyphal colonisation in the experimental cultivation setup and **(B)** contamination of the tubes after the end of the 1st period. Values show estimated marginal means ± standard error calculated from the linear model. Upper letters show significantly different groups based on Tukey's post-hoc test.

Verdier *et al.* 2014; Oei 2016) as well. This contamination was significantly treatment-dependent (LM: $F_{5,54} = 34.56$, p<0.0001; Fig. 6B, see Supplementary Data). Normal, non-treated tubes (N), and autoclaved tubes inoculated with microbial suspension or its cell-free filtrate (AM and AF) showed significantly lower infections than tubes with no microbiome or microbial metabolites (A, AW, and AA). It was already observed by Gyurkó (1978) that microbes have a protective role in *P. ostreatus* production, and bacteria may produce antifungal compounds against moulds in *Agaricus* mushroom production substrate (Liu *et al.* 2015). Velázquez-Cedeño *et al.* (2004) showed that on a straw-based cultivation substrate, bacteria reduced the competitive ability of *Trichoderma longibrachiatum* against *P. ostreatus*. In a later study (Velázquez-Cedeño *et al.* 2008), *Bacillus* spp. and *Paenibacillus polymyxa* were identified as the taxa responsible for these effects. This finding is consistent with our findings, as large amounts of Firmicutes bacteria were found in the mature substrate (Fig. 5, day 1 samples). Our results also unambiguously showed that this protective role was developed not only by the microbial community, but also by their secreted metabolites. Antifungal activity of microbe cell-free supernatants has been observed in several cases (Shehata *et al.* 2019; Xu *et al.* 2019), but this is the first time that it has been described during *P. ostreatus* production. Another important outcome is that inoculation with a single antagonistic *Bacillus* sp. (AA) neither reduced hyphal growth nor prevented contamination of the tubes.

Enzymatic activity of P. ostreatus
In the case of the 25 uninoculated control tubes and non-colonized region of the inoculated tubes, higher enzymatic activities (namely 1,4-β-xylosidase and endo-1,4-β-xylanase, Fig. S7, Supporting Information) were measured only in tubes characterised by higher contamination ratios (A, AW, and AA), which can be explained by the hemicellulose degrading capacity of *Aspergillus* sp. and *Penicillium* sp. (Andlar *et al.* 2018). In the non-colonized regions of normal, untreated tubes only activities close to detection limits were measured, showing that the microbial community of mature substrate prior to spawning with *P. ostreatus* had a negligible effect on measured enzymatic activities. Thus, for further analysis, only the enzymatic activity values of *P. ostreatus*-colonised regions were used, taking into account the effect of contamination.

To test the effects of different treatments on the enzymatic activities, new independent summary variables were created from original enzymatic activities with PCA for the 1st and 2nd periods separately (Table S3a, Supporting Information). Based on the effect of contamination, a new explanatory variable was introduced as 'treatment type' with two categories for treatments having higher (A, AA, and AW) and lower (AM, AF, and N) contamination values. According to the linear mixed-effects model, the combination of regions in model tubes and treatment type were the best explanatory variables (Table 3b, Supporting Information; Fig. 7). The significant effect of the regions was due to enzymatic activities of *P. ostreatus* in the cultivation model (Fig. S7, Supporting Information) showing a similar temporal trend as in the large-scale cultivation system (Bánfi *et al.* 2015). In the 1st period, during substrate colonisation, lignin-degrading enzymes were dominant, laccase in the region of front hyphae and MnP in the 3-week-old colonised parts. Treatment type slightly modified the actual values within a region. Unlike large-scale production, xylanases showed higher activity in the region of front hyphae, but only in the case of treatments with higher contamination. Thus, xylanases were produced, or xylanases were induced by the contaminating fungi. After inducing fruiting body production, during the 2nd period, high cellulose, xylan, and chitin-degrading enzyme activity were measured. Activities were similar in the two regions (recently and older colonised), but significantly different according to treatment type (Table S3b, Supporting Information; Fig. 7), so *P. ostreatus* showed higher activity in case of lower contamination (AM, AF, and N).

Potential role of bacteria during Pleurotus ostreatus production
Our results from large-scale mushroom production showed that the bacterial community composition of the mature mushroom substrate changed significantly during *P. ostreatus* production. DNA-based methods used did not reflect the activity of the given taxon, that is, whether the detected bacterium has an active role during mushroom production. However, modest community transformation during substrate colonisation and fruiting body production compared to substrate production (Fig. 3C), and the 5–10-fold reduction in relative bacterial 16S rRNA levels observed in a similar cultivation model (Vajna, Frey-Klett and Deveau 2013) support the idea of reduced bacterial activity in general, but does not exclude the active role of some selected lineages.
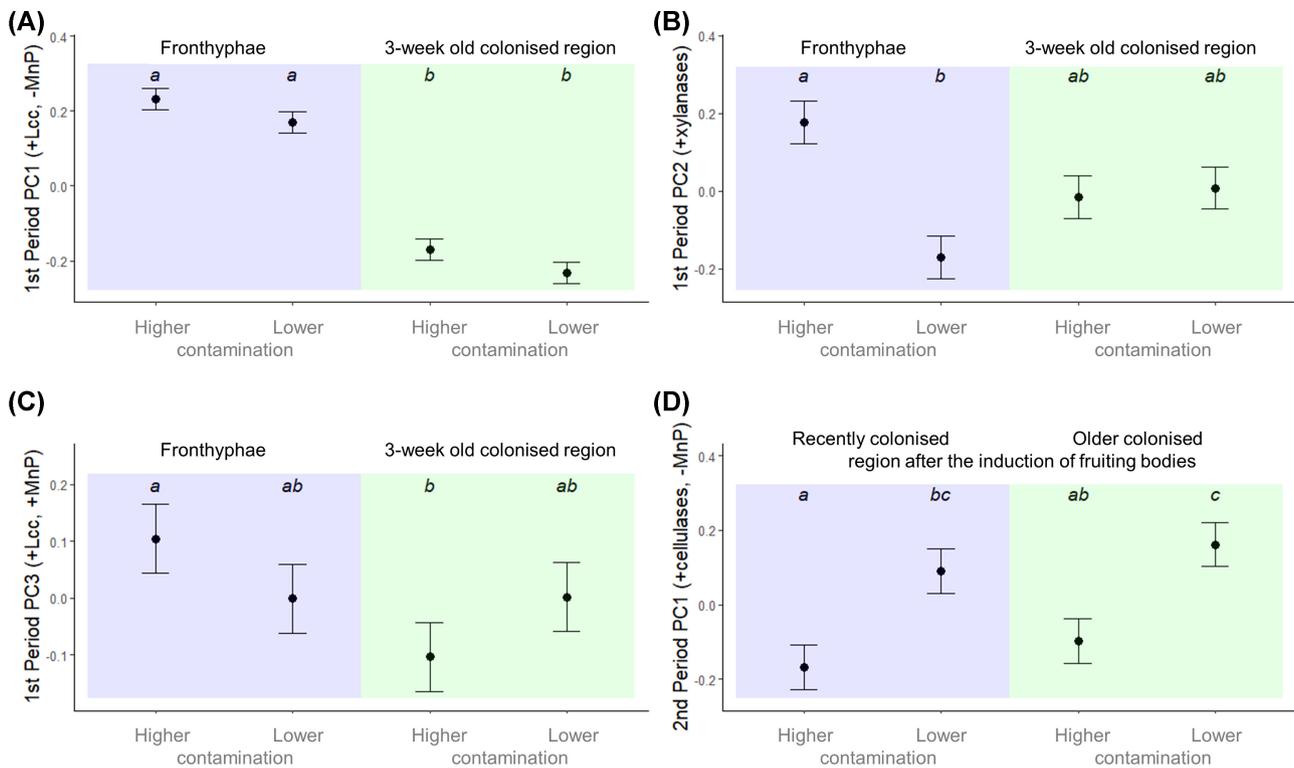
Figure 7. Enzymatic activities in the experimental cultivation setup: Effects of regions and different treatment types on the new PCA-derived summary variables in **(A-C)** 1st and **(D)** 2nd period. To understand which enzymes have a large impact on the respective principal components, see loadings in Table 3. 'Treatment type' was introduced based on LM for contamination and has two categories: treatments having higher (A, AA, and AW) and lower (AM, AF, and N) contamination ratios (For codes of the original treatments see Fig. 2A). Values show estimated marginal means ± standard error calculated from linear mixed-effects model. Upper letters show significantly different groups based on Tukey's post-hoc test. Lcc stands for laccase and MnP for manganese peroxidase.

In order to elucidate the role of microbes, the cultivation model was used to determine how the presence and absence of the known bacterial community affects *P. ostreatus* growth. Our main result was that the presence of microbes or their cell-free filtrate significantly decreased mushroom substrate contamination, and increased carbohydrate utilisation of *P. ostreatus* during fruiting body production. It is an important information from *P. ostreatus* producers, that proper substrate production (partial composting, pasteurisation, and conditioning) and consequently adequate microbial community is needed to avoid substrate contamination and because of this potential yield loss. It is worth mentioning that role of microbes is dependent on the mushroom species. In case of *Agaricus bisporus* primordia formation requires the presence of *Pseudomonas putida* or a related pseudomonad (Kertesz and Thai 2018).

Microbes play an important role prior to *P. ostreatus* colonisation, that is, they produce antimicrobial compounds (Nagy *et al.* 2012) during substrate production, which decrease the potential of later infection by competitive microbes. They also increase the accessibility of celluloses (Vajna *et al.* 2010). To test whether some microbe exert further activities during mushroom colonisation and fruiting body formation, or just survive in an inactive form (Mcgee *et al.* 2017), metaproteomic studies (Alessi *et al.* 2017) and analysis of secreted metabolites (Pinu *et al.* 2018; Senges *et al.* 2018) would be required.

increasing dominance of the order Bacillales and *Halomonas* spp., and decreasing relative abundance of *Thermus* spp. and Actinobacteria was described. In a cultivation model, it was proven that the presence of these microbes or their cell-free filtrate significantly decreased substrate contamination and increased cellulase and hemicellulase activity of *P. ostreatus* during fruiting body production. These findings support the hypothesis that the bacterial microbiome plays an important role prior to *P. ostreatus* spawning (e.g. by production of antimicrobial compounds, increase the accessibility of celluloses), and later *P. ostreatus* can use microbes partially to build their own biomass, but the microbes or their cell-free filtrate have a role in inhibiting competing microbes without hindering *P. ostreatus* growth.

SUPPLEMENTARY DATA

Supplementary data are available at *FEMSEC* online.

ACKNOWLEDGEMENTS

CONCLUSIONS

A definite succession of bacterial community composition during colonisation and fruiting body production of *P. ostreatus* with

FUNDING

REFERENCES

Abdo Z, Schüette UME, Bent SJ et al. Statistical methods for characterizing diversity of microbial communities by analysis of terminal restriction fragment length polymorphisms of 16S rRNA genes. *Environ Microbiol* 2006;**8**:929–38.

Adamski M, Pietr SJ. Biodiversity of bacteria associated with eight *Pleurotus ostreatus* (Fr.) P. Kumm. strains from Poland, Japan and the USA. *Pol J Microbiol* 2019;**68**:71–81.

Alessi AM, Bird SM, Bennett JP et al. Revealing the insoluble metasecretome of lignocellulose-degrading microbial communities. *Sci Rep* 2017;**7**:1–10.

Altschul SF, Gish W, Miller W et al. Basic local alignment search tool. *J Mol Biol* 1990;**215**:403–10.

Andersson BE, Lundstedt S, Tornberg K et al. Incomplete degradation of polycyclic aromatic hydrocarbons in soil inoculated with wood-rotting fungi and their effect on the indigenous soil bacteria. *Environ Toxicol Chem* 2003;**22**:1238–43.

Andlar M, Rezić T, Marđetko N et al. Lignocellulose degradation: an overview of fungi and fungal enzymes involved in lignocellulose degradation. *Eng Life Sci* 2018;**18**:768–78.

Baldrian P. Increase of laccase activity during interspecific interactions of white-rot fungi. *FEMS Microbiol Ecol* 2004;**50**:245–53.

Bánfi R, Pohner Z, Kovács J et al. Characterisation of the large-scale production process of oyster mushroom (*Pleurotus ostreatus*) with the analysis of succession and spatial heterogeneity of lignocellulolytic enzyme activities. *Fungal Biology* 2015;**119**:1354–63.

Barron GL. Microcolonies of bacteria as a nutrient source for lignicolous and other fungi. *Can J Bot* 1988;**66**:2505–10.

Beltran-Garcia MJ, Estarron-Espinosa M, Ogura T. Volatile compounds secreted by the oyster mushroom (*Pleurotus ostreatus*) and their antibacterial activities. *J Agric Food Chem* 1997;**45**:4049–52.

Berns AE, Philipp H, Narres HD et al. Effect of gamma-sterilization and autoclaving on soil organic matter structure as studied by solid state NMR, UV and fluorescence spectroscopy. *Eur J Soil Sci* 2008;**59**:540–50.

Cho YS, Kim JS, Crowley DE et al. Growth promotion of the edible fungus *Pleurotus ostreatus* by fluorescent pseudomonads. *FEMS Microbiol Lett* 2003;**218**:271–6.

Clausen CA. Bacterial associations with decaying wood: a review. *Int Biodeterior Biodegrad* 1996;**37**:101–7.

Cortes-Tolalpa L, Norder J, van Elsas JD et al. Halotolerant microbial consortia able to degrade highly recalcitrant plant biomass substrate. *Appl Microbiol Biotechnol* 2018;**102**:2913–27.

De Boer W, Folman LB, Klein Gunnewiek PJA et al. Mechanism of antibacterial activity of the white-rot fungus *Hypholoma fasciculare* colonizing wood. *Can J Microbiol* 2010;**56**:380–8.

De La Haba RR, Arahal DR, Sánchez-Porro C et al. The family Halomonadaceae. *The Prokaryotes: Gammaproteobacteria*. Vol 9783642389221. Springer-Verlag, Berlin Heidelberg, 2014, 325–60.

Deng Y, Wang R, Wang Y et al. Diversity and succession of microbial communities and chemical analysis in dried *Lutianus erythropterus* during storage. *Int J Food Microbiol* 2020;**314**:108416.

Deveau A, Bonito G, Uehling J et al. Bacterial-fungal interactions: ecology, mechanisms and challenges. *FEMS Microbiol Rev* 2018;**42**:335–52.

Felföldi T, Jurecska L, Vajna B et al. Texture and type of polymer fiber carrier determine bacterial colonization and biofilm properties in wastewater treatment. *Chem Eng J* 2015;**264**:824–34.

Folman LB, Klein Gunnewiek PJA, Boddy L et al. Impact of white-rot fungi on numbers and community composition of bacteria colonizing beech wood from forest soil. *FEMS Microbiol Ecol* 2008;**63**:181–91.

Gardes M, Bruns TD. ITS primers with enhanced specificity for basidiomycetes - application to the identification of mycorrhizae and rusts. *Mol Ecol* 1993;**2**:113–8.

Gramss G, Voigt KD, Kirsche B. Degradation of polycyclic aromatic hydrocarbons with three to seven aromatic rings by higher fungi in sterile and unsterile soils. *Biodegradation* 1999;**10**:51–62.

Gyurkó P. Die Rolle der Bakterien bei der Vorbereitung des Substrates für Pleurotus-Anbau. *Mushroom Sci* 1978;**10**:31–6.

Hervé V, Ketter E, Pierrat JC et al. Impact of *Phanerochaete chrysosporium* on the functional diversity of bacterial communities associated with decaying wood. *PLoS One* 2016;**11**:1–17.

Janusz G, Pawlik A, Świderska-Burek U et al. Laccase properties, physiological functions, and evolution. *Int J Mol Sci* 2020;**21**:966.

Jasińska A. Spent mushroom compost (SMC) – retrieved added value product closing loop in agricultural production. *Acta Agraria Debreceniensis* 2018;**150**:185–202.

Johnston SR, Boddy L, Weightman AJ. Bacteria in decomposing wood and their interactions with wood-decay fungi. *FEMS Microbiol Ecol* 2016;**92**:1–12.

Johnston SR, Hiscox J, Savoury M et al. Highly competitive fungi manipulate bacterial communities in decomposing beech wood (*Fagus sylvatica*). *FEMS Microbiol Ecol* 2019;**95**:1–13.

Kertesz MA, Thai M. Compost bacteria and fungi that influence growth and development of *Agaricus bisporus* and other commercial mushrooms. *Appl Microbiol Biotechnol* 2018;**102**:1639–50.

Kielak AM, Scheublin TR, Mendes LW et al. Bacterial community succession in pine-wood decomposition. *Frontiers in Microbiology* 2016;**7**:1–12.

Kim WG, Weon HY, Seok SJ et al. In vitro antagonistic characteristics of Bacilli isolates against *Trichoderma* spp. and three species of mushrooms. *Mycobiology* 2008;**36**:266.

Kovács J, Kovács S, Magyar N et al. Classification into homogeneous groups using combined cluster and discriminant analysis. *Environmental Modelling & Software* 2014;**57**:52–9.

Kwon H. Bottle cultivation. *Mushroom Grow Handb* 2004;**1**:166–71.

Lane DJ. 16S/23S rRNA sequencing. In: Stackebrandt E, Goodfellow M (eds). *'Nucleic acid techniques in bacterial systematics'* 1991, 15–751.

Lang, Lang E, Kleeberg I et al. Competition of *Pleurotus* sp. and *Dichomitus squalens* with soil microorganisms during lignocellulose decomposition. *Bioresour Technol* 1997;**60**:95–9.

Liu C, Sheng J, Chen L et al. Biocontrol activity of *Bacillus subtilis* isolated from *Agaricus bisporus* mushroom compost against pathogenic fungi. *J Agric Food Chem* 2015;**63**:6009–18.

Martínez MA, Ramírez DO, Simental SS *et al*. Antibacterial activity of spent substrate of mushroom *Pleurotus ostreatus* enriched with herbs. *J Agric Sci* 2015;**7**:225–31.

Mata JA, Béjar V, Llamas I *et al*. Exopolysaccharides produced by the recently described halophilic bacteria *Halomonas ventosae* and *Halomonas anticariensis*. *Res Microbiol* 2006;**157**:827–35.

Mcgee CF, Byrne H, Irvine A *et al*. Diversity and dynamics of the DNA and cDNA-derived bacterial compost communities throughout the *Agaricus bisporus* mushroom cropping process. *Annals of Microbiology* 2017;**67**:751–61.

Messner K, Fackler K, Lamaipis P *et al*. Overview of white-rot research: where we are today. *ACS Symposium Series* 2003;**845**:73–96.

Nagy A, Manczinger L, Tombácz D *et al*. Biological control of oyster mushroom green mould disease by antagonistic *Bacillus* species. *Biol Control Fungal Bact Plant Pathog* 2012;**78**:289–93.

Oei P. *Mushroom Cultivation IV*. 4th ed.In:Oei P (ed). Amsterdam: ECO Consult Foundation, 2016.

Ororbia MÁM, Núñez JP. La preparación del substrato. In: Sánchez JE, Royse DJ (eds.). *La Biología y El Cultivo de Pleurotus Spp*. Chiapas: El Colegio de la Frontera Sur, 2001, 157–86.

Pinu FR, Granucci N, Daniell J *et al*. Metabolite secretion in microorganisms: the theory of metabolic overflow put to the test. *Metabolomics* 2018;**14**.

Pruesse E, Peplies J, Glöckner FO. SINA: accurate high-throughput multiple sequence alignment of ribosomal RNA genes. *Bioinformatics* 2012;**28**:1823–9.

Quast C, Pruesse E, Yilmaz P *et al*. The SILVA ribosomal RNA gene database project: improved data processing and web-based tools. *Nucleic Acids Res* 2013;**41**:D590–6.

R Core Team. R: A Language and Environment for Statistical Computing. 2020.

Royse DJ, Baars J, Tan Q. Current overview of mushroom production in the world. *Edible and Medicinal Mushrooms*. John Wiley & Sons, Ltd, 2017, 5–13.

Rühl M, Kües U. Mushroom production. In: Kües U . *Wood production, wood technology, and biotechnological impacts*. Göttingen: Universitätsverlag Göttingen, 2007, 555–86.

Sağir A, Yildiz A. Growth of mycelium of *Pleurotus* spp. on different grains and determination of their competition with some contaminant fungi. *Acta Alimentaria* 2004;**33**:249–57.

Schloss PD, Westcott SL, Ryabin T *et al*. Introducing mothur: open-source, platform-independent, community-supported software for describing and comparing microbial communities. *Appl Environ Microbiol* 2009;**75**:7537–41.

Senges CHR, Al-Dilaimi A, Marchbank DH *et al*. The secreted metabolome of *Streptomyces chartreusis* and implications for bacterial chemistry. *Proc Natl Acad Sci* 2018;**115**:2490–5.

Shehata MG, Badr AN, El Sohaimy SA *et al*. Characterization of antifungal metabolites produced by novel lactic acid bacterium and their potential application as food biopreservatives. *Annals of Agricultural Sciences* 2019;**64**:71–8.

Smolskaite L, Venskutonis PR, Talou T. Comprehensive evaluation of antioxidant and antimicrobial properties of different mushroom species. *LWT - Food Science and Technology* 2015;**60**:462–71.

Stella T, Covino S, Čvančarová M *et al*. Bioremediation of long-term PCB-contaminated soil by white-rot fungi. *J Hazard Mater* 2017;**324**:701–10.

Suarez C, Ratering S, Weigel V *et al*. Isolation of bacteria at different points of *Pleurotus ostreatus* cultivation and their influence in mycelial growth. *Microbiol Res* 2019;**234**:126393.

Szabó A, Korponai K, Kerepesi C *et al*. Soda pans of the Pannonian steppe harbor unique bacterial communities adapted to multiple extreme conditions. *Extremophiles* 2017;**21**:639–49.

Székely AJAJ, Sipos R, Berta B *et al*. DGGE and T-RFLP analysis of bacterial succession during mushroom compost production and sequence-aided T-RFLP profile of mature compost. *Microb Ecol* 2009;**57**:522–33.

Tabachnick BG, Fidell LS. *Using Multivariate Statistics*. 6th ed. Boston: Pearson Education, Inc., 2013.

Vajna B, Frey-Klett P, Deveau A. Transcriptional and enzymatic profiling of *Pleurotus ostreatus* laccases and manganese peroxidases during mushroom cultivation. *Bacterial-Fungal Interactions: A Federative Field for Fundamental and Applied Microbiology* 2013;9.

Vajna B, Nagy A, Sajben E *et al*. Microbial community structure changes during oyster mushroom substrate preparation. *Appl Microbiol Biotechnol* 2010;**86**:367–75.

Vajna B, Szili D, Nagy A *et al*. An improved sequence-aided T-RFLP analysis of bacterial succession during oyster mushroom substrate preparation. *Microb Ecol* 2012;**64**:702–13.

Velázquez-Cedeño M, Farnet AM, Mata G *et al*. Role of *Bacillus* spp. in antagonism between *Pleurotus ostreatus* and *Trichoderma harzianum* in heat-treated wheat-straw substrates. *Bioresour Technol* 2008;**99**:6966–73.

Velázquez-Cedeño MA, Farnet AM, Ferré E *et al*. Variations of lignocellulosic activities in dual cultures of *Pleurotus ostreatus* and *Trichoderma longibrachiatum* on unsterilized wheat straw. *Mycologia* 2004;**96**:712–9.

Verdier T, Coutand M, Bertron A *et al*. A review of indoor microbial growth across building materials and sampling and analysis methods. *Build Environ* 2014;**80**:136–49.

Viziteu G. Cereal straw and corncobs. *Mushroom Grow Handb* 2004;**1**:86–90.

Vos AM, Heijboer A, Boschker HTS *et al*. Microbial biomass in compost during colonization of *Agaricus bisporus*. *AMB Express* 2017;**7**:12.

Vreeland RH, Anderson R, Murray RGE. Cell wall and phospholipid composition and their contribution to the salt tolerance of *Halomonas elongata*. *J Bacteriol* 1984;**160**:879–83.

White T, Bruns T, Lee S *et al*. Amplification and direct sequencing of fungal ribosomal RNA genes for phylogenetics. *PCR Protocols a Guide to Methods and Applications*. San Diego: Academic Press, 1990, 315–22.

Xu W, Wang H, Lv Z *et al*. Antifungal activity and functional components of cell-free supernatant from *Bacillus amyloliquefaciens* LZN01 inhibit *Fusarium oxysporum* f. sp. niveum growth. *Biotechnology & Biotechnological Equipment* 2019;**33**:1042–52.

Zhong XZ, Zeng Y, Wang SP *et al*. Insight into the microbiology of nitrogen cycle in the dairy manure composting process revealed by combining high-throughput sequencing and quantitative PCR. *Bioresour Technol* 2020;**301**:122760.